Human tau accumulation promotes glycogen synthase kinase-3β acetylation and thus upregulates the kinase: A vicious cycle in Alzheimer neurodegeneration

Qiuzhi Zhou,[a,1] Shihong Li,[a,1] Mengzhu Li,[a] Dan Ke,[a] Qun Wang,[a] Ying Yang,[a] Gong-Ping Liu,[a] Xiao-Chuan Wang,[a] Enjie Liu,[b]* and Jian-Zhi Wang [a,c]**

[a]Department of Pathophysiology, School of Basic Medicine, Key Laboratory of Education Ministry of China/Hubei Province for Neurological Disorders, Tongji Medical College, Huazhong University of Science and Technology, Wuhan 430030, China
[b]Department of Pathology, the First Affiliated Hospital of Zhengzhou University, Zhengzhou 450052, China
[c]Co-innovation Center of Neuroregeneration, Nantong University, Nantong 226000, China

eBioMedicine 2022;78: 103970
Published online xxx
https://doi.org/10.1016/j.ebiom.2022.103970

Summary

Background Glycogen synthase kinase-3β (GSK-3β) is one of the most effective kinases in promoting tau hyperphosphorylation and accumulation in Alzheimer's disease (AD). However, it is not clear how GSK-3β activity is regulated during AD progression.

Methods We firstly used mass spectrometry to identify the acetylation site of GSK-3β, and then established the cell and animal models of GSK-3β acetylation. Next, we conducted molecular, cell biological and behavioral tests. Finally, we designed a peptide to test whether blocking tau-mediated GSK-3β acetylation could be beneficial to AD.

Findings We found that GSK-3β protein levels increased in the brains of AD patients and the transgenic mice. Overexpressing tau increased GSK-3β protein level with increased acetylation and decreased ubiquitination-related proteolysis. Tau could directly acetylate GSK-3β at K15 both *in vitro* and *in vivo*. K15-acetylation inhibited ubiquitination-associated proteolysis of GSK-3β and changed its activity-dependent phosphorylation, leading to over-activation of the kinase. GSK-3β activation by K15-acetylation in turn exacerbated the AD-like pathologies. Importantly, competitively inhibiting GSK-3β K15-acetylation by a novel-designed peptide remarkably improved cognitive impairment and the AD-like pathologies in 3xTg-AD mice.

Interpretation Tau can directly acetylate GSK-3β at K15 which reveals a vicious cycle between tau hyperphosphorylation and GSK-3β activation.

Funding This study was supported in parts by grants from Science and Technology Committee of China (2016YFC1305800), Hubei Province (2018ACA142), Natural Science Foundation of China (91949205, 82001134, 31730035, 81721005), Guangdong Provincial Key S&T Program (018B030336001).

Keywords: Glycogen synthase kinase-3β; Alzheimer's disease; Tau; Acetylation; Proteolysis; Inhibitory peptide

Introduction

The activation of glycogen synthase kinase-3β (GSK-3β), which is highly expressed in central nervous system, plays a pivotal role in Alzheimer's disease (AD)[1]. The activity of GSK-3β is significantly increased in the brain and plasma of AD patients.[1–3] To the two hallmark pathologies observed in the AD brains, GSK-3β promotes the production of β-amyloid (Aβ) by up-regulating β-amyloid cleaving enzyme-1 (BACE1) and presenilin-1 (PS1) and mediates the toxicity of Aβ.[4–6] GSK-3β upregulation also induces tau hyperphosphorylation, damages neuronal synaptic plasticity,[7–10] and

*Corresponding author.
**Corresponding author at: Department of Pathophysiology, School of Basic Medicine, Key Laboratory of Education Ministry of China/Hubei Province for Neurological Disorders, Tongji Medical College, Huazhong University of Science and Technology, Wuhan 430030, China.
E-mail addresses: liuenjie01@163.com (E. Liu), wangjz@mail.hust.edu.cn (J.-Z. Wang).
[1] These authors contributed equally to this work.

Research in context

Evidence before this study

The activation of glycogen synthase kinase-3β (GSK-3β), which is highly expressed in central nervous system, plays a pivotal role in Alzheimer's disease (AD). The activity of GSK-3β is significantly increased in the brain and plasma of AD patients or AD transgenic mice. However, the mechanism underlying the abnormal upregulation of GSK-3β in AD remains largely unclear. We observed in a previous study that overexpressing tau remarkably increased GSK-3β enzyme activity. A recent study showed that tau had acetyltransferase activity and could induce its self-acetylation. We found that tau could acetylate β-catenin and thus stabilize β-catenin to mediate the anti-apoptosis function of tau. Thus, we speculate that tau may directly acetylate GSK-3β.

Added value of this study

In the present study, we demonstrated that tau could directly acetylate GSK-3β at K15 both *in vitro* and *in vivo*. Acetylation of GSK-3β at K15 by tau inhibited its ubiquitination-related proteolysis and changed its activity-dependent phosphorylation, which together upregulated the kinase activity. We also found that GSK-3β K15-acetylation exacerbated synaptic damages, neuroinflammation, tau hyperphosphorylation and Aβ production on the bases of wild-type GSK-3β, and ultimately led to cognitive impairments in mice. Importantly, inhibiting GSK-3β K15-acetylation by a designed peptide remarkably attenuated tau pathologies with improved synaptic and cognitive functions

Implications of all the available evidence

Tau could directly acetylate GSK-3β at K15 which reveal a vicious cycle between tau and GSK-3β, these finding not only uncovers a new mechanism underlying the chronic-worsening nature during AD progression but also provides promising drug candidate for AD.

causes spatial memory impairment.[11–15] GSK-3β damages neuronal function by promoting inflammation.[16–18] Inhibiting GSK-3β improves synaptic and cognitive functions in the AD-like mouse models.[11–15] However, the mechanism underlying the abnormal upregulation of GSK-3β in AD remains largely unclear.

Intracellular accumulation of microtubule-associated protein tau forming neurofibrillary tangles is one of the hallmark pathologies in AD.[19] The originally characterized function of tau is to promote microtubule assembly and maintain the stability of the microtubules.[20,21] Abnormal tau accumulation in the brain and cerebrospinal fluid are positively correlated with the degree of cognitive dysfunction in AD patients.[22–24] Overexpressing human tau in transgenic mice or wild-type mice induces synaptic damages and memory deficits,[25–28] and tau pathology closely tracks changes in brain function that are responsible for the onset of early symptoms in AD.[29] Reducing endogenous tau can improve excitotoxicity and cognitive impairment caused by Aβ.[30,31] Interestingly, we coincidently observed in a previous study that overexpressing tau remarkably increased GSK-3β enzyme activity.[32] Meanwhile, another study showed that knockout tau attenuated Aβ-induced GSK-3β activation.[33] GSK-3β undergoes a variety of post-translational modifications, which regulates the kinase activity and protein stability.[34–37] A recent study showed that tau had acetyltransferase activity and could induce its self-acetylation.[38] We found that tau could acetylate β-catenin and thus stabilize β-catenin to mediate the anti-apoptosis function of tau.[32,39] It is also reported that tau can interact with GSK-3β.[40,41] Based on these observations, we speculate that tau may directly acetylate GSK-3β, by which it upregulates GSK-3β activity and thereby forms a vicious circle to cause chronic neurodegeneration as observed in the AD progression.

In the present study, we demonstrated that tau could directly acetylate GSK-3β at K15 both *in vitro* and *in vivo*. Acetylation of GSK-3β at K15 by tau inhibited its ubiquitination-related proteolysis and changed its activity-dependent phosphorylation, which together upregulated the kinase activity. We also found that GSK-3β K15-acetylation exacerbated synaptic damages, neuroinflammation, tau hyperphosphorylation and Aβ production on the bases of wild-type GSK-3β, and ultimately led to cognitive impairments in mice. Importantly, inhibiting GSK-3β K15-acetylation by a designed peptide remarkably attenuated tau pathologies with improved synaptic and cognitive functions.

Methods

Plasmids, viruses, antibodies, chemicals, transgenic mice, and human brain tissue

The plasmid pEGFP-Tau-2N4R (Tau40), encoding human tau, was a generous gift of Dr. Fei Liu (Jiangsu Key Laboratory of Neuroregeneration, Nantong, China). The plasmid of Tau-k18(-) (Tau40 protein lacking microtubule-binding repeats domain (243–372)) was generated by PCR and cloned in an EGFP C1 vector in ECORI and BamHI restriction sites. The plasmids of pCDNA3.0-HA-GSK-3β WT/K15R/K27R/K205R and EGFPC1-GSK-3β WT/ K15Q were carried out using the Mut Express II Fast Mutagenesis Kit by following the manufacturer's instructions (Cat#: C214-01, Vazyme Biotech, Nanjing, China) based on the plasmid pCDNA3.0-GSK-3β WT. The AAV-CaMKII-eGFP-2A-vector-3xFlag, AAV-CaMKII-eGFP-2A-GSK-3β WT-3xFlag, AAV-CaMKII-eGFP-2A-GSK-3β K15Q-3xFlag and AAV-Syn-eGFP-Tau40 was purchased from OBio Biologic Technology Co., Ltd. All the antibodies were validated and used in Table S2. Cycloheximide (Chx) was from Sigma-Aldrich (St. Louis, MO, USA).

TPOP146 and L-45 dihy-drochloride (L-45) were from MedChemExpress (Cat#: HY-100697, HY-101125, Shanghai, China). Scrambled peptide (FAQKEPSCVQ-RRRRRRRR), P1 (FAESCKPVQQ-RRRRRRRR) and P2 (PRTTSFAESCKPVQQPSAFGS-RRRRRRRR) were synthesized by Haode Peptide (Wuhan, China). Bicinchoninic Acid Protein Detection Kit was from Sigma-Aldrich. CCK-8 kit was from MedChemExpress (Cat#: HY-K0301, Shanghai, China). Reagents for cell culture were from Gibco (Grand Island, NY, USA).

Male C57BL/6 mice (2-month-old, 20−30 g) were purchased from the Experimental Animal Central (Beijing Vital River Laboratory Animal Technology Co., Ltd.). The human tau transgenic mice (RRID: IMSR_JAX:004808, STOCK Mapttm1(EGFP)Klt Tg (MAPT)8cPdav/J, stock number 004808), tau knockout mice (RRID: IMSR_JAX:004779, STOCK Mapttm1 (EGFP)Klt/J, stock number 004779), 3xTg-AD transgenic mice (RRID:IMSR_JAX:031988,129S4.Cg-Tg (APPSwe,tauP301L)1LfaPsen1tm1Mpm/LfaJ, stock number 031988) and APP/PS1 transgenic mice (B6C3-Tg(APPswe,PSEN1dE9)85Dbo/Mmjax, Stock number 034829, RRID:IMSR_JAX:031988) were from Jackson laboratory. All mice were kept at 24 ± 2°C with accessible food and water under a 12 h light/dark cycle. Brain tissue and sections from 12-month male hTau mice and the age-matched male tau knockout mice, 9-month female 3xTg and the age-matched female wild-type 129 mice, and 8-month male APP/PS1 mice and the age-matched male wild-type C57 mice were used for Ace-GSK-3β K15 western blotting and immunostaining. 2-month male C57 mice were used for virus injection. 12-month female 3xTg or age-matched female wild-type mice were used for peptide administration. Only mice weighing 20−30 g were used in all the experiments. The random number generator was used to divide the experimental animals into control and treatment groups. Mice were removed if they died abnormally or deteriorated in the course of the experiment. All animal experiments were performed according to the "Policies on the Use of Animals and Humans in Neuroscience Research" revised and approved by the Society for Neuroscience in 1995, and the Guidelines for the Care and Use of Laboratory Animals of the Ministry of Science and Technology of the People's Republic of China, and the Institutional Animal Care and Use Committee at Tongji Medical College, Huazhong University of Science and Technology approved the study protocol. Postmortem human brain samples were provided by Dr. Chao Ma of Human Brain Bank, Chinese Academy of Medical Sciences. Subjects information, including age, sex and postmortem interval, were listed in Table S1.

Cell culture, transfection, and drug treatment

Human embryonic kidney 293 cells (HEK293, RRID: CVCL_0045, Cat#: GDC0067, China Center for Type Culture Collection) were cultured in 90% DMEM/High Glucose medium containing 10% FBS, in a humidified atmosphere of 5% CO_2 at 37 °C. Mouse neuroblastoma N2a cells (N2a, RRID: CVCL_0470, Cat#: GDC0162, China Center for Type Culture Collection) were cultured in 45% DMEM/High Glucose medium and 45% Opti-MEM containing 10% FBS, in a humidified atmosphere of 5% CO_2 at 37 °C. HEK293 and N2a cell lines have been validated. The cell lines were tested for mycoplasma and the result was negative. Transfection of plasmids in cells was carried out with Neofect^{TM} DNA transfection reagent kit (Cat#: TF20121201, Neofect Biotech, Beijing, China) by following the manufacturer's instructions. Chx (100 μg/mL) was used to inhibit protein biosynthesis at different time points. TPOP146 (134 nM) and L-45 dihydrochloride (126 nM), dissolved in DMSO (0.1%), were used to inhibit respectively the activity of CBP/P300 and PCAF. For inhibiting GSK-3β K15 residue acetylation, peptides were dissolved in phosphate buffer saline (PBS), and administrated into the medium for 48 h.

Primary hippocampal neuron culture was performed as described before,[39] neurons were isolated from 17d- to 19d-embryonic Sprague Dawley rats. Hippocampus was isolated and neurons were planted with the F-12 medium containing 10% FBS on a coverslip in a 12-well plate with 20,000 cells per well or on a 6-well plate with 100,000 cells per well. Four hours after plating, medium was replaced with 1.5 ml of fresh maintenance medium containing 97% neurobasal medium, 2% B27, and 1% GlutaMAX. At 5 div, neurons were infected with lentivirus with a multiplicity of infection (MOI) of 10. Half of the maintenance medium was changed every 3 days.

Cell viability analysis

Cell viability was assessed using CCK-8 kit by following the manufacturer's instructions. The cells were seeded at a concentration of 5000 cells per well in a 96-well plate and then treated with various concentrations of P1/2 respectively (0, 25, 50, 75, 100 μM) for 48 h. After the treatments, the culture medium was removed, and 10 μL of CCK-8 in 90 μL of medium was added. After incubating for 30 min at 37 °C, the absorbance was measured at 450 nm using a microplate reader (BioTek, 250058).

In test-tube acetylation assays

For the in test-tube acetylation assay performed as described before,[39] The recombinant Tau and GSK3β were purified by using prokaryocyte (E. coli) expressing system. The cDNAs of Tau and GSK-3β were cloned respectively in a GST-His-tagged PET-41a(+) vector and cultured in Rosetta2(de3)pLysS competent cells, and then affinity-purified by using Ni-NTA resin. 50 nM each of the

purified Tau proteins, 2 μM each of the purified GSK-3β, and 1 mM acetyl CoA (Sigma) were incubated at 37 °C for 2 h with constant shaking. The reaction buffer contains 50 mM HEPES (pH 8.0), 1 mM dithiothreitol (DTT), 10% glycerol and 10 mM sodium butyrate. The acetylation level of GSK-3β was analyzed by Western blotting using anti-acetylated lysine antibody. The immunoreactive bands were quantified by using the Odyssey Infrared Imaging System (LI-COR Biosciences, Lincoln, NE, USA) or ECL Imaging System (610007-8Q, Clinx Science Instruments Co., Ltd). Michaelis−Menten parameters were determined using GraphPad Prism 6.

RT-qPCR

Total RNA was isolated by using Trizol™ kit (Cat#: 15596026, Invitrogen, Carlsbad, CA, USA) and the reverse transcription reagent kit (Cat#: RR037, Takara) was used to obtain cDNA. RT−PCR was performed using a StepOnePlus Real-Time PCR Detection System (AB Applied Biosystems, 272001262, Cossell Biotechnology). The PCR system contains 2 μL forward and reverse primers, 10 μL SYBR Green PCR master mixes (Cat#: Q711-02, Vazyme, Nanjing), 1 μL cDNA and 7 μL diethylpyrocarbonate (DEPC H_2O). The primer information is as follows:

GSK-3β-Mus-F: TCCCCGAGGAAAAATATAATACTCA
GSK-3β-Mus-R: CTGCCATCTTTATCTCTGCTAACT
GSK-3β-Rattus-F: GTATGGTCTGCTGGCTGTGT
GSK-3β-Rattus-R: AAGAGTGCAGGTGTGTCTCG
β-actin-Mus-F: TATAAAACCCGGCGGCGCA
β-actin-Mus-R: TCATCCATGGCGAACTGGTG
β-actin-Rattus-F: ACCCGCCACCAGTTCGC
β-actin-Rattus-R: CACGATGGAGGGGAAGACG

Construction of endogenous GSK-3β knockout cell line

For the construction of endogenous GSK-3β knockout cell line, gRNA is used to cause a DNA double-strand break in the gene region where the GSK-3β acetylation site is located, with the CRISPR/Cas9 system, to achieve endogenous GSK-3β knockout in HEK293 cells.

Afterward, monoclonal selection was performed from the endogenous GSK-3β knock-out cell pool, and the genomic DNA and total protein of the selected monoclonal cell lines were extracted by PCR amplification and sequencing and Western blotting.

gRNA sequence: CGGCTTGCAGCTCTCCGCAAAGG
Sequence of PCR primers for sequencing:
Forward sequence: AATATCCGTGCCGATCTG
Reverse sequence: GCTGCTTCATCCTTGACT

Mass spectrometric analysis

For mass spectrometric analysis, we first prepared GSK-3β by immunoprecipitation using anti-GSK-3β from HEK293 cells which were transfected with Tau40 for 48 h, followed by western blotting. After coomassie blue staining, gel bands were manually excised. Then, the gel bands were completely decolorized and lyophilized, and were incubated with 40 μl trypsin buffer at 37 °C for 16−18 h. Subsequently, the protein sample was separated using a nanoliter flow rate HPLC liquid phase system Easy nLC 1200. Solvents were prepared as follows: Liquid A was 0.1% formic acid aqueous solution and liquid B was 0.1% formic acid acetonitrile solution. The chromatographic column was equilibrated with 95% of the A solution. The sample was loaded from the autosampler to the mass spectrometry pre-column C18trap column (C18 3 mm 0.10 × 20 mm) and then separated by the analytical column C18 column (C18 1.9 mm 0.15 × 120 mm) with a flow rate of 600 nl/min. The sample was separated by capillary high-performance liquid chromatography and analyzed by mass spectrometry using a Q-Exactive mass spectrometer (Thermo Scientific).

Cell viability analysis

Cell viability was assessed using CCK-8 kit by following the manufacturer's instructions (Cat#: HY-K0301, Shanghai, China). The cells were seeded at a concentration of 5000 cells per well in a 96-well plate and then treated with various concentrations of P1/2 respectively (0, 25, 50, 75, 100 μM) for 48 h. After the treatments, the culture medium was removed, and 10 μL of CCK-8 in 90 μL of medium was added. After incubating for 30 min at 37 °C, the absorbance was measured at 450 nm using a microplate reader (Bio-Tek, 250058).

Western blotting

The cells were collected and were lysed for 30 min on ice in RIPA buffer, and then centrifuged at 12,000 × g for 15 min at 4°C. The hippocampal/ hippocampal CA1 tissues were homogenized with RIPA buffer on ice and centrifuged at 12,000 × g for 15 min at 4°C. The supernatant was collected and the protein levels were analyzed using bicinchoninic acid (BCA, KF016, Sigma-Aldrich) by following the manufacturer's instructions. And then the lysate was mixed with loading buffer (3:1, vol/vol) containing 200 mM Tris-HCl, pH 6.8, 8% SDS, 40% glycerol, and boiled for 10 min. After SDS/PAGE, the protein was transferred onto nitrocellulose membranes (Whatman) and then incubated with primary antibodies at 4°C for overnight. Incubation of secondary antibodies was performed at room temperature for 1 h and visualized using the ECL Imaging System (610007-8Q, Clinx Science Instruments Co., Ltd).

Immunoreactive bands were quantitatively analyzed by Image J2x software.

Immunohistochemistry

For immunohistochemical studies, mice were anesthetized and then perfused through the aorta with 0.9% normal saline followed by phosphate buffer containing 4% paraformaldehyde. Brains were removed and post-fixed in perfusate overnight and then immersed into 30% (wt/vol) sucrose liquid diluted with PB twice for about 3 days. Once sinking to the bottom of the tubes, brains were snap frozen at −80 °C and then cut for slices (30 μm) with a freezing microtome. The brain slices were washed with PBS containing 0.1% Triton X-100 (PBST) for 3×5 min, followed by 3% H_2O_2 diluted in PBS for 30 min. After washing with PBST for 3×5 min, the brain slices were blocked with 5% BSA for 30 min at room temperature. Then slices were incubated with primary antibodies overnight at 4°C. After washing with PBST three times, immunoreaction was developed using the Polink-2 plus® Polymer HRP Detection kit (ZSGB-BIO, PV-9001/PV9002) and visualized with diaminobenzidine (brown color). Slices were sequentially dehydrated in 50%, 75%, 95% and 100% ethanol for 6 times (20 min each) and cleared in xylene for 3 times (30 min each) and cover-slipped with Permount solution. Images were obtained with a microscope (Olympus BX60, Tokyo, Japan).

Immunofluorescence

The cultured cells were fixed in 4% (wt/vol) paraformaldehyde for 30 min at room temperature. Brain slices and cultured cells were permeabilized in 0.5% Triton X-100 (vol/vol) diluted in PBS solution. Nonspecific binding sites were blocked via incubating in 5% (wt/vol) BSA containing 0.1% Triton X-100 (vol/vol) for 30 min at room temperature. The samples were incubated with primary antibodies at 4°C overnight, followed by washing 3 times in PBST and subsequent incubation with secondary antibodies for 1 h at 37°C and counterstained with DAPI. Finally, samples were washed and mounted onto slides with 50% glycerin-PBS (vol/vol) solution. All the slides were imaged with a confocal microscope (Zeiss Carl LSM 780, Germany).

GSK-3β activity assay

The activity of GSK-3β was assayed using a kit (Cat#: GMS50161.6, Genmed) by following the manufacturer's instructions as reported before.[42] In brief, the cells were collected and were lysed in GENMED lysis buffer (Reagent B). 130 μL GenMed buffer solution (Reagent C), 20 μL GenMed enzymatic solution (Reagent D), 20 μL GenMed reaction solution (Reagent E), and 20 μL GenMed substrate solution (Reagent F) were added into each well successively and were incubated at 30°C for 3min. 100 μg protein sample or Negative solution (Reagent G, 10 μL) were added into a well, and immediately placed into the enzyme plate for detection. Relative GSK-3β activity were calculated according to the following formula: [(5 min absorbance − 0 min absorbance) × sample dilution factor × 0.1]/[0.005 × 6.22 (absorbance fraction) × 0.5 × reaction time].

Spine analyses

The spine image acquisition and analysis were performed as described in a previous study.[43] The neurons expressing non-fused GFP were used for spine counting. A Zeiss 100× immersion objective (Zeiss LSM710, Carl Zeiss AG, Oberkochen, Germany) was used to acquire images with 0.5 μm z-resolution. Spine densities refer to the number of spines per 10 μm dendrite length analyzed by using Image J2x software.

Electrophysiological recordings

Mice used for electrophysiology experiments were deeply anesthetized as described above. When all pedal reflexes were abolished, brains were removed and placed in ice-cold oxygenated slicing solution containing the following: 225 mM sucrose, 3 mM KCl, 1.25 mM NaH_2PO_4, 24 mM $NaHCO_3$, 6 mM $MgSO_4$, 0.5 mM $CaCl_2$, and 10 mM D-glucose. Coronal slices (300 μm thick) were cut at 4−5 °C in the slicing solution using a Leica VT1000S vibratome and then transferred to an incubation chamber filled with oxygenated slicing solution in a 30°C water bath for 1 h before being recorded. For LTP, slices were laid down in a chamber with an 8 × 8 microelectrode array in the bottom planar (each 50 × 50 μm in size, with an interpolar distance of 150 μm) and kept submerged in artificial cerebrospinal fluid (aCSF; 1−2 mL/min) with a platinum ring glued by a nylon silk. Signals were acquired using the MED64 System (Alpha MED Sciences, Panasonic). The fEPSPs were recorded by stimulating the Schaeffer fibers. LTP was induced by applying three trains of high-frequency stimulation (HFS; 100 Hz, 1s duration). LTP magnitude was calculated as the average (normalized to baseline) of the responses recorded 50-60 min after conditioning stimulation. All the signals were recorded by using the MED64 System.

Stereotaxic surgery

For stereotaxic surgery, the 2-month-old C57BL/6 mice were placed in a stereotaxic apparatus and anesthetized with 2% isoflurane (RWD Life Science, R510-22) through a nose cone (300−500 mL/min, RWD Life Science, China, R500). Then, AAV-CaMKII-eGFP-2A-vector-3xFlag or AAV-CaMKII-eGFP-2A-GSK-3β WT-3xFlag or AAV-CaMKII-eGFP-2A-GSK-3β K15Q-3xFlag (1 μl, 4.0 × 10^{12} viral particles per ml) was bilaterally

injected into the hippocampal CA1 region (posterior 1.82 mm, lateral 1.0 mm, and ventral 1.25 mm relative to bregma) at a rate of 0.1 μL/min. The needle was kept in place for 10 min before withdrawal. After the skin was sutured, the mice were placed on a heater for analepsia.

For *in vivo* peptide administration, guiding cannulas (RWD, Shenzhen, China) were implanted into the lateral ventricle (posterior 0.22 mm, lateral ± 1.0mm from the bregma, ventral -2.5 from the skull) of 12-month-old S129 mice and 3xTg mice, the peptides (1mM, 5 μL) were delivered using an automatic microinjection system (World Precision Instruments, USA), once every 2 days. Mice were restricted in a custom-designed device and stayed awake during drug administration. Upon deep anaesthesia (loss of the pedal pain, slowing of breathing and heart rate), these mice were euthanized by excising the heart for further analysis after behavioral experiments.

Sucrose preference test

For the sucrose preference test, the three groups of mice were first adapted to drinking water from two bottles for three days. Then mice were placed in separate cages, and water was removed from the cages for 24 h; Then two bottles were given to mice for drinking 2 h and the water in one of the bottles was replaced with 2% sucrose solution. To avoid side preferences, the two bottles were switched each 1h. Percent sucrose preference was calculated as drinking volume of sucrose solution/ (drinking volume of sucrose solution + drinking volume of water) x 100%.

Open field test

The mice are placed in the room the day before the behavioral test to acclimate to the environment, each mouse is marked and placed in order, and the experiment is performed in the order of marking and placement, and all subsequent behavioral experiments follow this pattern. The Open field test consisted of a 5 min session in a quadrate chamber (white opaque plastic), which was divided into 16 square regions, a central field (center 4 square regions) and a periphery field. Each mouse was placed in the same position at the start of the test. Behaviors were recorded and analyzed by the video tracking system (Chengdu Taimeng Software Co., Ltd, China).

Novel object recognition test

The novel object recognition test was carried out according to the procedure reported.[44] The mice were habituated to a quadrate chamber (white opaque plastic) for 5 min without objects 24 h before the test. The chamber was cleaned with 75% ethanol between each habituation period. The day after the mice re-entered the chamber from the same starting point and were given 10 min to familiarize themselves with object A and object B. After each period the chamber and objects were cleaned with 75% ethanol. The next day after the familiarization period, object B was replaced with novel object C, and the mice were given 10 min to explore both objects. The exploring time on each object was recorded. The recognition index was calculated by TC/(TA+TC) and the discrimination index was calculated by (TC-TA)/(TA+TC). TA, TC were respectively the time mice exploring the object A and C. Behaviors were recorded and analyzed by the video tracking system (Chengdu Taimeng Software Co., Ltd, China).

Elevated plus maze test

The EPM apparatus consisted of two open arms (66 cm × 6 cm) and two closed arms (66 cm × 6 cm) connected by a junction area (6 cm × 6 cm), at a height of 50 cm above the ground. Mice were placed at the junction of the four arms of the maze facing an open arm. And the duration time in each arm was recorded for 5 min by the video tracking system (Chengdu Taimeng Software Co., Ltd, China). An increase in open arm activity (duration) reflects anti-anxiety behavior. Between each trial, the maze was cleaned with 75% ethanol.

Morris water maze test

The spatial learning and memory were assessed by Morris water maze (MWM) performed as described before.[39] The maze was divided into 4 quadrants with a platform placed in one quadrant. The mice were trained to find the hidden platform for 6 consecutive days, 3 trials per day. In each training trial, the mouse started from one of four quadrants facing the wall of the pool and the trial ended when the animal climbed on the platform. If mice failed to locate the platform within 60 s, they were gently guided onto the platform and stayed there for 30 s; the escape latency was recorded as 60 s. The spatial memory was tested 1 day after the last training. Mice were allowed to explore the water maze for 60 s with the platform removed. The latency to reach the target quadrant, target platform crossings and the time spent in the target quadrant were recorded by a digital video camera connected to a computer (Chengdu Taimeng Software Co. Lid, China).

Fear conditioning test

Mice were placed into a square chamber with a grid floor. On the first day (day 1), each mouse was habituated to the chamber for 3 min, and then a foot shock (0.9 mA, 3 s) was delivered. Three sequential foot shocks at 3-min intervals were applied. Then the mice were returned to their home cages. On the next day (day 2), the mice were exposed to the same chamber without

any stimulus for 3 min. The contextual conditioning was assessed by recording freezing behavior during the 3min exposure. Freezing time during the 3 min was recorded for assessment of memory.

Ethics

All animal experiments were performed according to the "Policies on the Use of Animals and Humans in Neuroscience Research" revised and approved by the Society for Neuroscience in 1995, and the Guidelines for the Care and Use of Laboratory Animals of the Ministry of Science and Technology of the People's Republic of China, and the Institutional Animal Care and Use Committee at Tongji Medical College, Huazhong University of Science and Technology approved the study protocol ([2020] IACUC Number:2397).

Post-mortem human brain samples were provided by Dr. Chao Ma of Human Brain Bank, Chinese Academy of Medical Sciences. AD was diagnosed according to the criteria of the Consortium to Establish a Registry for AD and the National Institute on Aging. Approvals were from Medical Ethics Committee of Tongji Medical College, Huazhong University of Science and Technology. Informed consent was obtained from the subjects. ([2016] IEC Number: S182)

Statistical analysis

All data were collected and analyzed in a blinded manner. Data were analyzed using Graphpad software. All data conform to normal distribution after the Kolmogorov-Smirnov D test. Statistical analyses were performed using Student's t test for two-group comparisons or one-way or two-way ANOVA, followed by post hoc tests for multiple comparisons among more than two groups. The results were presented as mean ± SEM and $p < 0.05$ was accepted as statistically significant.

Role of the funding source

The funding sources had absolutely no involvement in the study design, collection, analysis and interpretation of data, manuscript preparation and the decision to submit the paper for publication.

Results

The AD-like tau accumulation increases GSK-3β acetylation and stabilizes the kinase

We previously observed that overexpressing tau activated GSK-3β,[32] but the mechanism has been unclear. Here, we first examined the levels of total and the phosphorylation GSK-3β in human tau transgenic mice. The result showed that the levels of total and the Tyr216-phosphorylated GSK-3β (active) were increased, while the level of Ser9-phosphorylated GSK-3β (inactive) was decreased in 12-month-old human tau transgenic mice compared with the endogenous tau knockout mice (Figure 1a–d). Overexpressing human Tau40 in the cultured primary hippocampal neurons increased GSK-3β protein level (Figure 1e,f). The mRNA level was not changed in human tau transgenic mice and the cultured primary hippocampal neurons (Figure 1g,h). These and the previous data together suggest that the AD-like tau accumulation upregulates GSK-3β activity by influencing its protein post-translational modifications but not at its gene expression level.

Previous studies show that acetylation of GSK-3β regulates its protein level and enzyme activity,[37] and tau has acetyltransferase activity.[38,39] Therefore, we speculate that tau may directly acetylate GSK-3β, and thus inhibit its protein degradation and upregulate the kinase activity. To prove this, we overexpressed Tau40, or its acetyltransferase activity domain-deleted Tau-K18 (-), or the empty vector in N2a cells, and measured the changes of GSK-3β. Overexpressing tau significantly increased GSK-3β total protein level (Figure 1i–k), the acetylation GSK-3β level detected by immunoprecipitation of GSK-3β and Western blotting using a pan-acetylation reactive antibody (Figure 1l,m). Overexpressing tau also increased the enzyme activity of GSK-3β (Figure 1p) with a simultaneously reduced ubiquitination and degradation of the kinase (Figure 1n,o,q,r) compared with the empty vector control, while expressing Tau-K18(-) abolished the above-mentioned effects of tau on GSK-3β (Figure 1i–r). These data together indicate that tau may upregulate GSK-3β by promoting its acetylation.

Tau can directly and dominantly acetylate GSK-3β at K15 leading to the kinase upregulation and the K15-acetylated GSK-3β is significantly increased in AD patients and the transgenic models

To explore the acetylation site(s) of GSK-3β, we first prepared GSK-3β by immunoprecipitation and used mass spectrometry. The results showed that acetylation of GSK-3β by tau was clustered at its N-terminal and the N-terminal sequence TTSFAESCKPVQQPSAFGSMKVSRD of GSK-3β is highly conserved in different species (Figure 2a,b). By site-specific mutagenesis of GSK-3β at lys15, lys27 and lys205 to acetylation-resistant arginine (K15R, K27R and K205R), we found that co-expressing K15R mutant almost abolished tau-induced acetylation, whereas mutation at K27R and K205R did not significantly change the acetylation level of GSK-3β (Figure 2c), suggesting that tau may dominantly acetylate GSK-3β at K15. Then, we developed an antibody against K15-acetylated GSK-3β and confirmed that the antibody only reacted with acetylated-GSK-3β but not the acetylation-resistant GSK-3β (K15R) (Figure S1a–c).

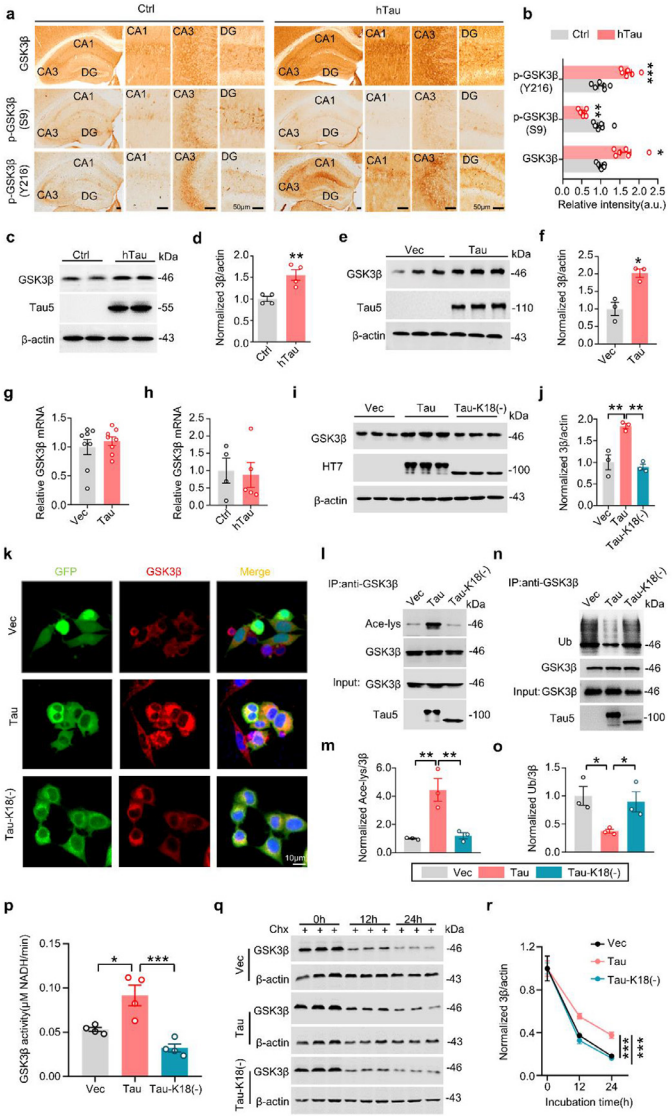

Figure 1. Overexpressing tau increases GSK-3β acetylation with inhibited ubiquitination and proteolysis of the kinase. (a−d) GSK-3β total protein level and pGSK-3β(Y216) (active form) increased and pGSK-3β(S9) (inactive form) decreased in the hippocampi of 12-month-old human tau transgenic mice (hTau) compared with the endogenous tau knockout mice (Ctrl) measured by Western blotting (c, d; $n = 4$ for each group, unpaired Student's t-test, $^{**}p < 0.01$ vs Tau-), and immunohistochemical staining (a,b), bar = 50 μm. ($n = 6$ for each group, $^{*}p < 0.05$, $^{**}p < 0.01$, $^{***}p < 0.001$vs Ctrl). (e,f) Overexpressing tau increased GSK-3β protein level in primary hippocampal neurons transfected with AAV-eGFP-Vector or AAV-eGFP-Tau at 7 div and cultured for another 5 div, measured by Western blotting. ($n = 3$ for each group, unpaired Student's t-test, $^{*}p < 0.05$ vs Vec). (g,h) Overexpressing tau did not affect mRNA level of GSK-3β in cultured primary hippocampal neurons (g) and the human tau transgenic mice (hTau) (h) detected by RT−PCR. (i−k) Expressing Tau-K18(-) abolished tau-induced GSK-3β upregulation in N2a cells transfected with empty Vec, or Tau40 or Tau-K18(-) for 48 h and then measured by Western blotting (i,j) or immunofluorescent staining (k). ($n = 3$ for each group, one-way ANOVA, $^{**}p < 0.01$ vs Tau, bar = 10 μm). (l−o) Expressing Tau-K18(-) abolished tau-induced GSK-3β acetylation (l,m) with restored ubiquitination (n,o) in N2a cells transfected with empty Vec, or Tau40 or Tau-K18(-) for 48 h and then measured by immunoprecipitation using anti-GSK-3β and Western blotting using anti-ace-lys or anti-Ub, anti-GSK-3β, and Tau5, respectively. ($n = 3$ for each group, one-way ANOVA, $^{*}p < 0.05$, $^{**}p < 0.01$ vs Tau). (p) Expressing Tau-K18(-) abolished tau-induced upregulation of GSK-3β activity in N2a cells measured by GSK-3β activity assay. ($n = 4$ for each group, one-way ANOVA, $^{*}p < 0.05$, $^{***}p < 0.001$ vs Tau). (q,r) Expressing Tau-K18(-) attenuated tau-induced inhibition of GSK-3β proteolysis. N2a cells were transfected with Vec, or Tau-40, or Tau-K18(-) for 24 h, and then treated with Cycloheximide (Chx) for 12 h or 24 h, followed by Western blotting. GSK-3β protein level was normalized to β-actin. ($n = 3$ for each group, two-way ANOVA, $^{***}p < 0.001$ vs tau). Data were presented as mean ± SEM.

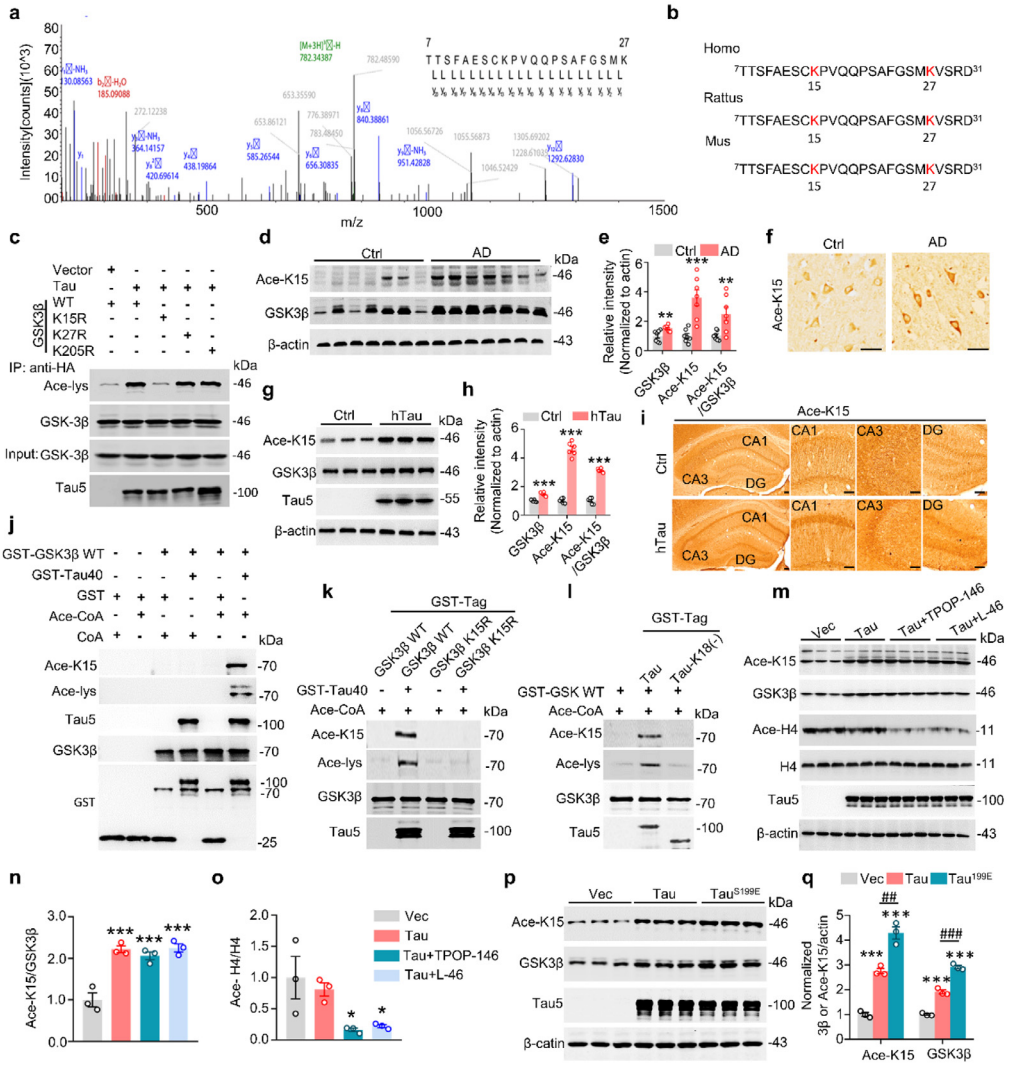

Figure 2. Tau can dominantly and directly acetylate GSK-3β at K15 and the K15-acetylated GSK-3β is remarkably increased in the brains of AD patients and the transgenic mice. (a,b) Tau acetylates GSK-3β at its N-terminal measured by immunoprecipitation using anti-GSK-3β in HEK293 cells transfected with Tau, followed by coomassie brilliant blue staining and then the band of 46 kDa was collected for mass spectrometry analysis, the N-terminal sequence of GSK-3β is highly conserved in different species. (c) Expressing K15-acetylation-resistant mutant (K15R) abolished tau-induced GSK-3β acetylation measured in HEK293 cells co-transfected with HA-GSK-3β (WT, or K15R, or K27R, or K205R) and tau or the empty Vector for 48 h, and then immunoprecipitated using anti-HA and Western blotting using anti-GSK-3β, anti-ace-lys, and Tau5, respectively. (d−f) The increased total GSK-3β and Ace-GSK-3β-K15 levels detected by Western blotting (d,e) and immunohistochemistry (f) in the hippocampal extracts of AD patients compared with age-matched controls. (n =7 for each group, unpaired Student's t-test, $^{**}p < 0.01$, $^{***}p < 0.001$ vs Ctrl, bar = 50 μm). (g−i) The increased GSK-3β K15-acetylation was detected in the hippocampal extracts of human tau transgenic mice (hTau) compared with endogenous tau knockout mice (Ctrl), measured by Western blotting (g, h) and immunohistochemistry (i) using acetylation site-specific antibody (Ace-GSK-3β-K15, ace-K15). (n = 6 for each group, unpaired Student's t-test, $^{**}p < 0.01$, $^{***}p < 0.001$ vs Ctrl, bar = 50μm). (j,k) Tau can directly acetylate GSK-3β measured by incubating affinity-purified GST-Tau40 and GST-GSK-3β or GST-GSK-3β-K15R in test-tube for *in vitro* acetylation assay and using an Ace-GSK-3β-K15-specific antibody for western blotting, and mutation of GSK-3β at K15 abolished its acetylation by tau. (The band shows GST fusion purified protein) (l) Deletion of Tau40 at acetyltransferase activity region abolished its acetylation activity on GSK-3β measured by incubation affinity purified GST-Tau40 or GST-TauK18(-) and GST-GSK-3β in test-tube for *in vitro* acetylation assay and using an Ace-GSK-3β-K15-specific antibody for western blotting. (The band shows GST fusion purified protein) (m−o) Inhibiting acetyltransferases CBP/P300 by TPOP146 (134 nM) or PCAF by L-45 (126 nM) for 24 h did not significantly decrease the K15-acetylated GSK-3β level in tau-overexpressing N2a cells measured by western blotting. (n = 3 for each group, one-way ANOVA, $^{*}p < 0.05$, $^{***}p < 0.001$ vs Vec). (p,q) Expressing pseudo-phosphorylated tau (Tau^{S199E}) further increased GSK-3β K15-acetylation in HEK293 cells transfected with Vec, Tau40, or Tau^{S199E} for 48 h. (n = 3 for each group, one-way ANOVA, $^{***}p < 0.001$ vs Vec, $^{\#\#}p < 0.01$, $^{\#\#\#}p < 0.001$ vs Tau). Data were presented as mean ± SEM.

By using this antibody, we also detected a significantly increased level of K15-acetylated GSK-3β in AD patients (Figure 2d–f) and the transgenic mouse and cell models, including human tau transgenic mice (Figure 2g–i), human tau-overexpressing N2a cells (Figure S2a,b), AAV-eGFP-tau transfected hippocampal neurons (12 div) (Figure S2c,d), 3xTg AD mice (Figure S2e–g), and APP/PS1 mice (Figure S2h–j). These data reveal an increased level of K15-acetylated GSK-3β in AD patients and the AD transgenic models.

To confirm the direct effect of tau on GSK-3β, we incubated purified tau and purified GSK-3β in the test-tube and then measured the acetylation level of GSK-3β. We confirmed that tau could directly acetylate GSK-3β (Figure 2j), while GSK-3β mutation at K15 (Figure 2k) or tau mutation at acetyltransferase activity region (Figure 2l) abolished the acetylation. To verify whether tau plays a dominant role in acetylating GSK-3β K15, we used inhibitors (TPOP146 and L-45) of CBP/P300 and PCAF. Reduction of the acetylated H4 (Ace-H4) confirmed the suppression of CBP/P300 and PCAF activity by TPOP146[45] or L-45.[46] However, inhibiting CBP/P300 only slightly decreased the acetylation level of K15-GSK-3β by tau (Figure 2m–o), which suggests a predominant role of tau in acetylating GSK-3β K15. We also observed that expressing pseudo-phosphorylated tau (Tau^{S199E}) further increased K15-acetylation compared with wild type tau (Figure 2p,q).

These data together demonstrate that tau can directly and dominantly acetylate GSK-3β at K15 and thus upregulate the kinase both *in vitro* and *in vivo*, and tau phosphorylation enhances its acetyltransferase activity toward GSK-3β.

GSK-3β K15-acetylation increases its kinase activity with inhibited ubiquitination and proteolysis

Phosphorylation of GSK-3β at serine 9 (pS9) inhibits the kinase, while at tyrosine 216 (pY216) activates the kinase.[47,48] To explore the effect of tau-induced GSK-3β acetylation on its activity, we mutated K15 to glutamine (Q) to mimic the lysine acetylation ($GSK\text{-}3\beta^{K15Q}$). We observed that expressing $GSK\text{-}3\beta^{K15Q}$ significantly increased pY216-GSK-3β and decreased pS9-GSK-3β in N2a cells and in mouse hippocampal CA1 (Figure 3a–d), suggesting the kinase activation by tau-induced acetylation. To confirm the role of GSK-3β K15-acetylation on its kinase activity, we generated a GSK-3β KO cell model by using CRISPR/Cas9 (Figure 3e), and then exogenously expressing wild-type GSK-3β ($GSK\text{-}3\beta^{WT}$) or $GSK\text{-}3\beta^{K15Q}$. We found that expressing $GSK\text{-}3\beta^{K15Q}$ significantly increased its enzymatic activity (Figure 3eF–G) with inhibited ubiquitination and degradation (Figure 3eH–K) compared with expressing $GSK\text{-}3\beta^{WT}$. $GSK\text{-}3\beta^{K15R}$ (mimic deacetylated GSK-3β) reversed the effect of $GSK\text{-}3\beta^{K15Q}$ on its kinase activity (Figure S1). These data confirm that GSK-3β K15-acetylation can activate the kinase with the mechanisms involving affecting the activity-dependent phosphorylation and ubiquitination-associated proteolysis of GSK-3β.

GSK-3β K15-mimic acetylation causes cognitive impairment

GSK-3β is postulated to play an important role in cognitive function and psychiatric behaviors.[43,49–51] To characterize the effects of GSK-3β K15-acetylation on the cognitive ability of mice, we stereotaxically injected adeno-associated virus (AAV) vectors carrying $GSK\text{-}3\beta^{WT}$ (AAV-$GSK\text{-}3\beta^{WT}$), $GSK\text{-}3\beta^{K15Q}$ (AAV-$GSK\text{-}3\beta^{K15Q}$), or the empty vector control with non-fusion eGFP into 2-month-old C57 mice hippocampal CA1 subset. After 1 month, GSK-3β overexpression in CA1 was confirmed by GFP imaging (Figure 4a) and Western blotting (Figure 4b).

Then, we measured the effect of GSK-3β K15Q on learning and memory by using novel object recognition (NOR), Morris water maze (MWM) and contextual fear-conditioning (FC), respectively. In NOR trial, both $GSK\text{-}3\beta^{WT}$ and $GSK\text{-}3\beta^{K15Q}$ mice showed decreased recognition index (Figure 4c) and discrimination index (Figure 4d) to the novel object, meaning that both GSK-3βWT and GSK-3β K15Q mice had memory impairments and the impairment was more significant in $GSK\text{-}3\beta^{K15Q}$ group than the $GSK\text{-}3\beta^{WT}$ group (Figure 4c and d). During learning trial in MWM test, the $GSK\text{-}3\beta^{K15Q}$ mice showed significant learning deficit evidenced by the longest latency at days 4, 5, and 6 compared with the $GSK\text{-}3\beta^{WT}$ and the empty vector groups (Figure 4e). These findings demonstrate that $GSK\text{-}3\beta^{K15Q}$ impairs spatial learning. During the memory test on day 8 by removing the platform, the $GSK\text{-}3\beta^{K15Q}$ group showed longest latency to reach the target quadrant (Figure 4f), the lowest crossings at the platform site (Figure 4g), and the shortest time spent in the target quadrant (Figure 4h) compared with the $GSK\text{-}3\beta^{WT}$ and the empty vector groups. No motor dysfunction was shown evaluated by swimming speed (Figure 4i). These results of MWM test suggested that $GSK\text{-}3\beta^{K15Q}$ expression impaired spatial memory. In FC test, $GSK\text{-}3\beta^{K15Q}$ mice showed decreased freezing time compared with $GSK\text{-}3\beta^{WT}$ and the empty vector groups (Figure 4j), meaning that $GSK\text{-}3\beta^{K15Q}$ mice have the worst freezing memory compared with other two groups. These results demonstrate that overexpressing $GSK\text{-}3\beta^{K15Q}$ induces or aggravates multiple cognitive deficits. Overexpressing $GSK\text{-}3\beta^{K15Q}$ also induced anxiety- and depression-like behaviors evidenced by sucrose preference (Figure 4k), open field (Figure 4l–n) and elevated plus-maze (Figure 4o) tests. Together, these results suggest that overexpressing K15 mimic acetylated GSK-3β can significantly lead to cognitive impairment and mood disorders.

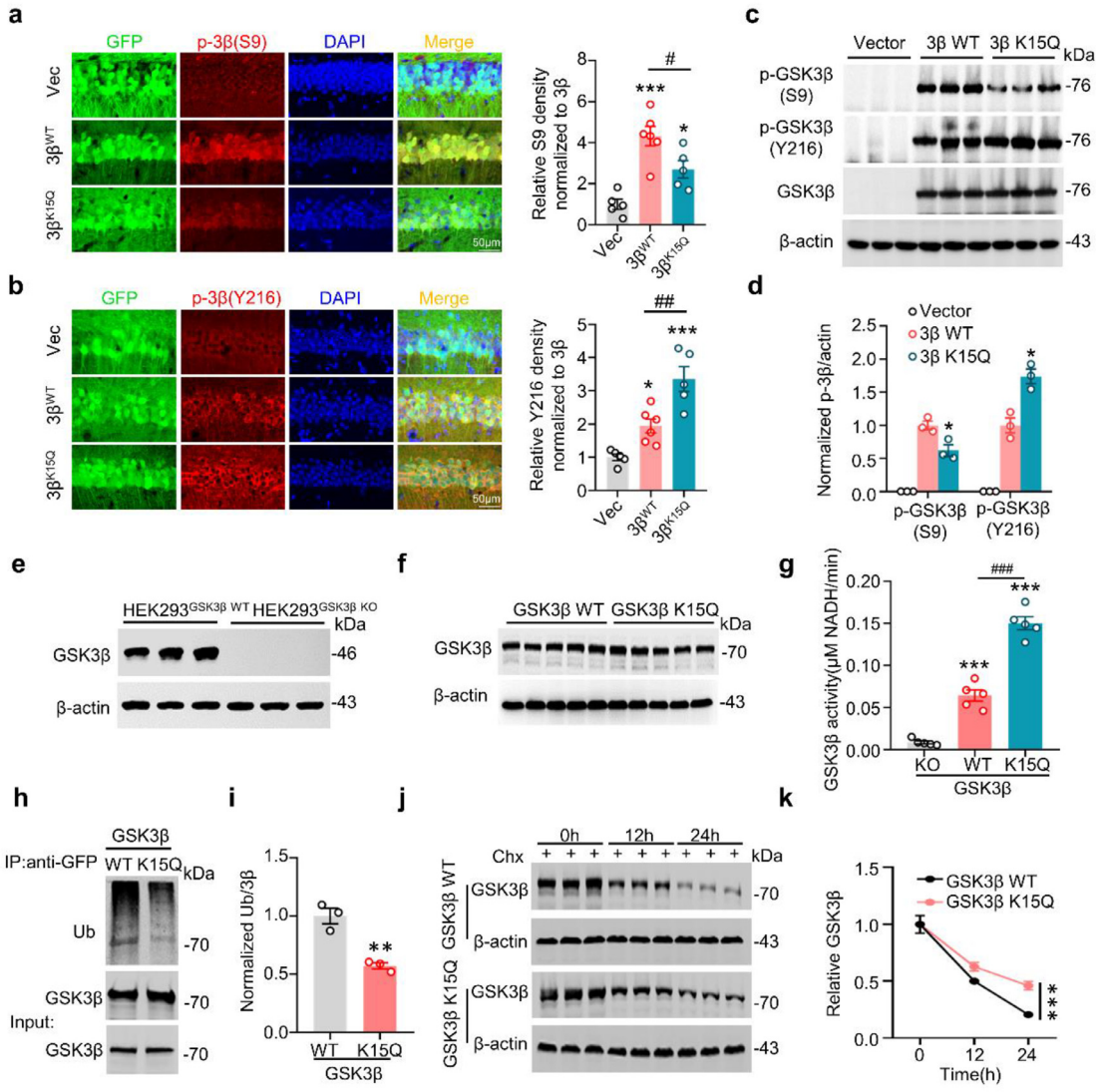

Figure 3. GSK-3β K15-acetylation increases its kinase activity with reduced ubiquitination and proteolysis. (a,b) K15-acetylation increases GSK-3β activity in mice. AAV-GSK-3β^{WT} or AAV-GSK-3β^{K15Q} was stereotaxically infused into the hippocampal CA1 of 2-month-old C57 mice for 1 month, and then levels of pS9-GSK-3β (inactive) and pY216-GSK-3β (active) in CA1 were measured by immunofluorescence and normalized to total GSK-3β. (n = 5-6 for each group, one-way ANOVA, *$p < 0.05$, ***$p < 0.001$ vs Vec, #$p < 0.05$, ##$p < 0.01$ vs 3β^{WT}, bar = 50 μm). (c,d) Empty-Vector, GFP-GSK-3β WT and GFP-GSK-3β K15Q plasmids were transfected into N2a cells, GSK-3β K15-mimic acetylation increased its kinase activity in N2a cells measured by Western blotting shown by decreased pS9-GSK-3β and increased pY216-GSK-3β (The band shows exogenously expressed GFP fusion protein). (n = 3 for each group, one-way ANOVA, *$p < 0.05$ vs GSK-3β WT). (e−g) GSK-3β K15-mimic acetylation increased its kinase activity measured by activity assay. GSK-3β was knocked out (KO) by using CRISPR/Cas9 assay and the expression of endogenous GSK-3β was verified by Western blotting (e), and re-expression of GFP-GSK-3β WT or GFP-GSK-3β K15Q plasmid in the KO cell model for 12 h and the exogenously expressed GFP fusion GSK-3β was verified by Western blotting (f) followed by GSK-3β activity assay (g). (n = 5 for each group, one-way ANOVA, ***$p < 0.001$ vs GSK-3β KO, ###$p < 0.001$ vs GSK-3β WT). (h,i) GSK-3β K15-mimic acetylation inhibited its ubiquitination. HEK293 cells were co-transfected with HA-ubiquitin and GFP-GSK-3β WT or GFP-GSK-3β K15Q plasmid for 24 h, and then GSK-3β was immunoprecipitated by anti-GFP and blotted by anti-Ub and anti-GSK-3β. (The band shows exogenously expressed GFP fusion protein). (n = 3 for each group, unpaired Student's t-test, **$p < 0.01$ vs GSK-3β WT). (j,k) GSK-3β K15-mimic acetylation inhibited its degradation. HEK293 cells were transfected with GFP-GSK-3β WT or GFP-GSK-3β K15Q plasmid for 24 h and then treated with cycloheximide (Chx,100 μg/ml) for 12 h or 24 h, and then measured the protein level of GSK-3β by western blotting. (The band shows exogenously expressed GFP fusion protein). (n = 3 for each group, two-way ANOVA, ***$p < 0.001$ vs GSK-3β WT, ###$p < 0.001$ vs GSK-3β K15R). Data were presented as mean ± SEM.

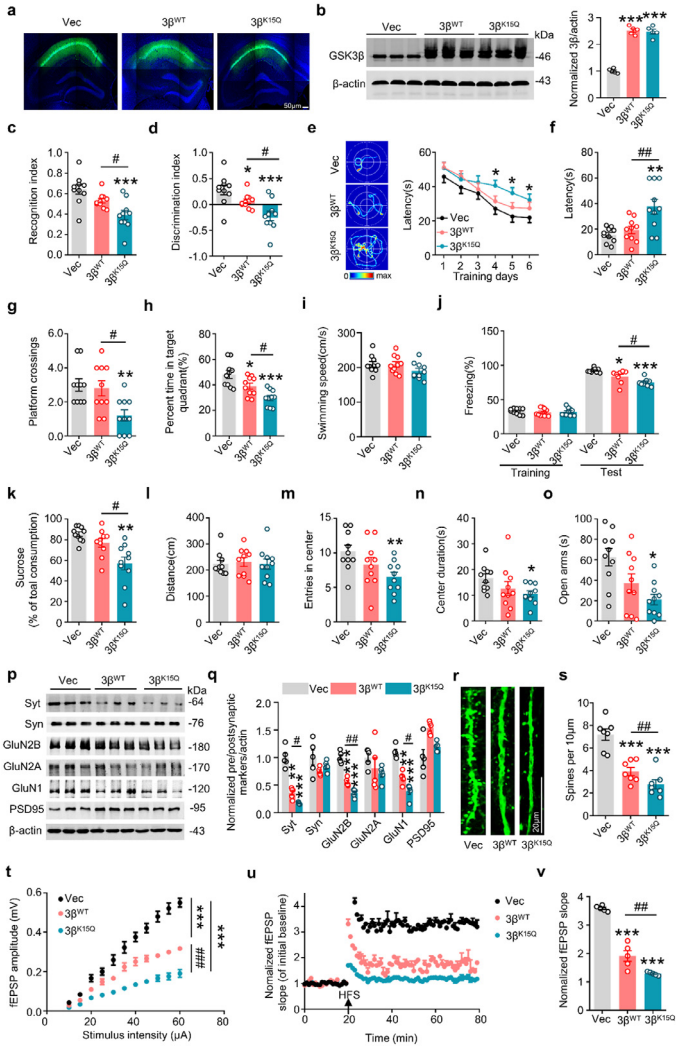

Figure 4. GSK-3β K15-acetylation causes memory impairment and synaptic dysfunction. (a) Representative image showing virus expression in hippocampal CA1 of 2-month-old C57 mice after stereotactic infusion for 1 month. (b) Infusion of AAV-GSK-3β^{WT} or AAV-GSK-3β^{K15Q} upregulated GSK-3β protein level compared with the AAV-Vector measured by Western blotting. (n = 5 for each group, one-way ANOVA, ***$p < 0.001$ vs Vec, bar = 50 μm). (c,d) Mice expressing GSK-3βK15Q had memory deficits shown by the decreased recognition index (c) and the discrimination index (d) recorded at 24 h after training during novel object recognition test. (n = 10 for each group, one-way ANOVA, *$p < 0.05$, ***$p < 0.001$ vs Vec, #$p < 0.05$ vs GSK-3β^{WT}). (e−i) Mice expressing GSK-3β^{K15Q} had spatial learning deficit shown by the increased latency to find the platform at days 4, 5, and 6 during Morris water maze training trial (e), and memory deficit shown by the increased latency to reach the target quadrant (f), decreased crossings in the platform site (g), and percent time in target quadrant (h) during probe trial done at day 8 by removed the platform; and the GSK-3β^{K15Q} mice did not show difference in swimming speed (i). (n = 10 for each group, one-way ANOVA, *$p < 0.05$, **$p < 0.01$, ***$p < 0.001$ vs Vec, #$p < 0.05$, ##$p < 0.01$ vs GSK-3β^{WT}). (j) The memory deficit in GSK-3β^{K15Q} mice was also detected by fear conditioning test shown by the lowest percent of freezing time. (n = 10 for each group, one-way ANOVA, *$p < 0.05$, ***$p < 0.001$ vs Vec, #$p < 0.05$ vs GSK-3β^{WT}). (k−o) Mice expressing GSK-3βK15Q showed anxiety-like behavior evidenced by the decreased sugar intake in water preference test (k), reduced entries and time in center with unchanged total moved distance in open field test (l-n), and decreased time spent in open arms during elevated plus-maze test (o). (n = 10 for each group, one-way ANOVA, *$p < 0.05$, **$p < 0.01$ vs Vec, #$p < 0.05$ vs GSK-3β^{WT}). (p,q) Mice expressing GSK-3β^{K15Q} showed significantly decreased levels of GluN2B, GluN1 and Syt with no change of GluN2A, PSD95 and Syn compared with GSK-3β^{WT} in the hippocampus. (n = 5 for each group, one-way ANOVA, **$p < 0.01$, ***$p < 0.001$ vs Vec, #$p < 0.05$, ##$p < 0.01$ vs GSK-3βWT). (r,s) Mice expressing GSK-3β^{K15Q} showed significant spine loss in GFP-positive neurons at hippocampal CA1. (n = 7 for each group, one-way ANOVA, ***$p < 0.001$ vs Vec, ##$p < 0.01$ vs GSK-3β^{WT}, bar = 20 μm). (t−v) Mice expressing GSK-3β^{K15Q} showed synaptic dysfunction demonstrated by the decreased input−output curve (t) and the decreased fEPSP slope induced by applying 3 trains of high-frequency stimulation (HFS) (u,v). (n = 5 mice for each group, one-way ANOVA, ***$p < 0.001$ vs Vec, ##$p < 0.01$, ###$p < 0.001$ vs GSK-3β^{WT}). Data were presented as mean ± SEM.

GSK-3β K15Q exacerbates synaptic plasticity impairment and AD-like pathologies

To explore the mechanisms that may underlie the behavioral impairments induced by GSK-3β K15-acetylation, we measured the levels of synapse-related proteins, spine density and morphology, and the functional synaptic transmission. By Western blotting, we observed that expressing GSK-3β^{K15Q} significantly decreased the levels of postsynaptic GluN2B and GluN1 and presynaptic synaptotagmin (Syt) without changing GluN2A, PSD95 and synaphysin1 (Syn) (Figure 4p,q). Simultaneously, the spine density was significantly decreased in GSK-3β^{K15Q} group compared with the GSK-3β^{WT} and the empty vector groups (Figure 4r,s). By *ex vivo* brain slice electrophysiological recording, we found that expressing GSK-3β^{K15Q} suppressed basal synaptic transmission as shown by a decreased input-output (I-O) curve (Figure 4t). The fEPSP slope was reduced in GSK-3β^{K15Q}-expressing slices compared with the GSK-3β^{WT} and the empty vector controls (Figure 4u,v). These data suggest overexpression of GSK-3β leads to impairment of synaptic plasticity, which is further exacerbated by K15 mimetic acetylation of GSK-3β.

We also observed that expressing GSK-3β^{K15Q} further increased tau phosphorylation at Ser202, Ser396 and Ser404 on the bases of GSK-3β^{WT} in mouse hippocampi measured by Western blotting (Figure 5a,b) and immunohistochemistry (Figure 5c). GSK-3β^{K15Q} exacerbated microglia and astrocyte activation (Figure 5d–g) with significantly increased cleavage of caspase-3 (Figure 5h,i) compared with GSK-3β^{WT}, while there was no difference on NeuN staining (Figure 5j,k). These data suggest that GSK-3β K15-acetylation-induced tau hyperphosphorylation and cell apoptosis also contribute to cognitive deficits.

Blocking tau-induced GSK-3β acetylation rescues cognitive impairment and the AD-like pathologies in 3xTg-AD mice

As shown above, tau accumulation increases GSK-3β K15-acetylation, which in turn aggravates tau hyperphosphorylation and synaptic dysfunction, leading to cognitive deficit. Therefore, blocking tau-mediated GSK-3β acetylation could be beneficial to AD. To verify this, we designed two peptides, named as P1 (FAESCKPVQQRRRRRRRR) and P2 (PRTTSFAESCKPVQQPSAFGS RRRRRRRR), respectively. The peptides contain homology sequence around K15 of GSK-3β with RRRRRRRR at its C-terminal for cell penetration. By CCK8 assay in HEK293 cells, we observed that application of P1 or P2 at concentrations no more than 100 μm did not induce any significant change in cell viability (Figure S4a,d). Then, we measured the effect of the peptides on inhibiting GSK-3β K15-acetylation in HEK293 cells with transient expression of human tau (eGFP-hTau). We observed that P1 treatment (100 μm) significantly decreased tau-induced GSK-3β K15-acetylation (Figure S4b,c), while P2 slightly attenuated GSK-3β K15-acetylation with similar pattern as P1 (Figure S4e, f). P1 (100 μm) also inhibited GSK-3β activity with reduced tau phosphorylation (Figure S4g,h). These *in vitro* data indicate that P1 can efficiently attenuate tau-induced GSK-3β K15-acetylation *in vitro* which in turn reduces tau pathologies.

To investigate the effects of P1 *in vivo*, we delivered P1 or scrambled peptide (1 mM in 5 μL) through a guiding cannula implanted into the lateral ventricle of 12-month-old 3xTg-AD/S129 mice once every two days for one month, and then measured the cognitive functions. In NOR trial, P1 treated mice showed increased recognition and the discrimination index to the novel object in 3xTg-AD mice (Figure 6a,b). In MWM training trial, P1 treated mice showed shorter latency at days 5 and 6 than the untreated group in 3xTg-AD mice (Figure 6c). In MWM probe trial, P1 treated mice showed increased platform crossings (Figure 6d) and target quadrant time (Figure 6e) with no changes in swimming speed (Figure 6f). P1 treatment also increased synapse-associated proteins (Figure 6g,h) and spine numbers (Figure 6i,j). No changes were shown by P1 treatment in open field test (Figure S5a, b) and fear memory test (Figure S5c). We also confirmed that P1 treatment significantly decreased GSK-3β K15-acetylation and its activity with decreased tau hyperphosphorylation in the hippocampi of 3xTg-AD mice measured by Western blotting (Figure 6k,l) and Immunofluorescence (Figure 6m). Additionally, P1 treatment significantly attenuated microglia and astrocyte activation (Figure S6a,b) with increased NeuN staining (Figure S6c).

These data together demonstrate that inhibiting GSK-3β K15-acetylation by a novel designed peptide can attenuate multiple AD-like pathologies and improve the cognitive impairments in 3xTg AD mice.

Discussion

Both GSK-3β and tau are intimately involved in AD pathogenesis. Most studies have been focused on GSK-3β as an upstream pathological promoter of tau, because it is one of the most active kinases in phosphorylating tau at multiple AD-associated sites. We previously observed that overexpressing tau activated GSK-3β enzyme activity,[32] implying that tau may act upstream of GSK-3β. In current study, we demonstrate that tau can directly and dominantly acetylate GSK-3β at K15, and the K15-acetylation of GSK-3β inhibits its ubiquitination and increases its activity. Based on these findings, we propose that a vicious cycle between tau hyperphosphorylation and GSK-3β activation eventually results in synaptic dysfunction which may underlie the memory deficit and the chronic nature during AD.

GSK-3β can be activated by an increased total level or its Tyr216-phosphorylation and GSK-3β can be

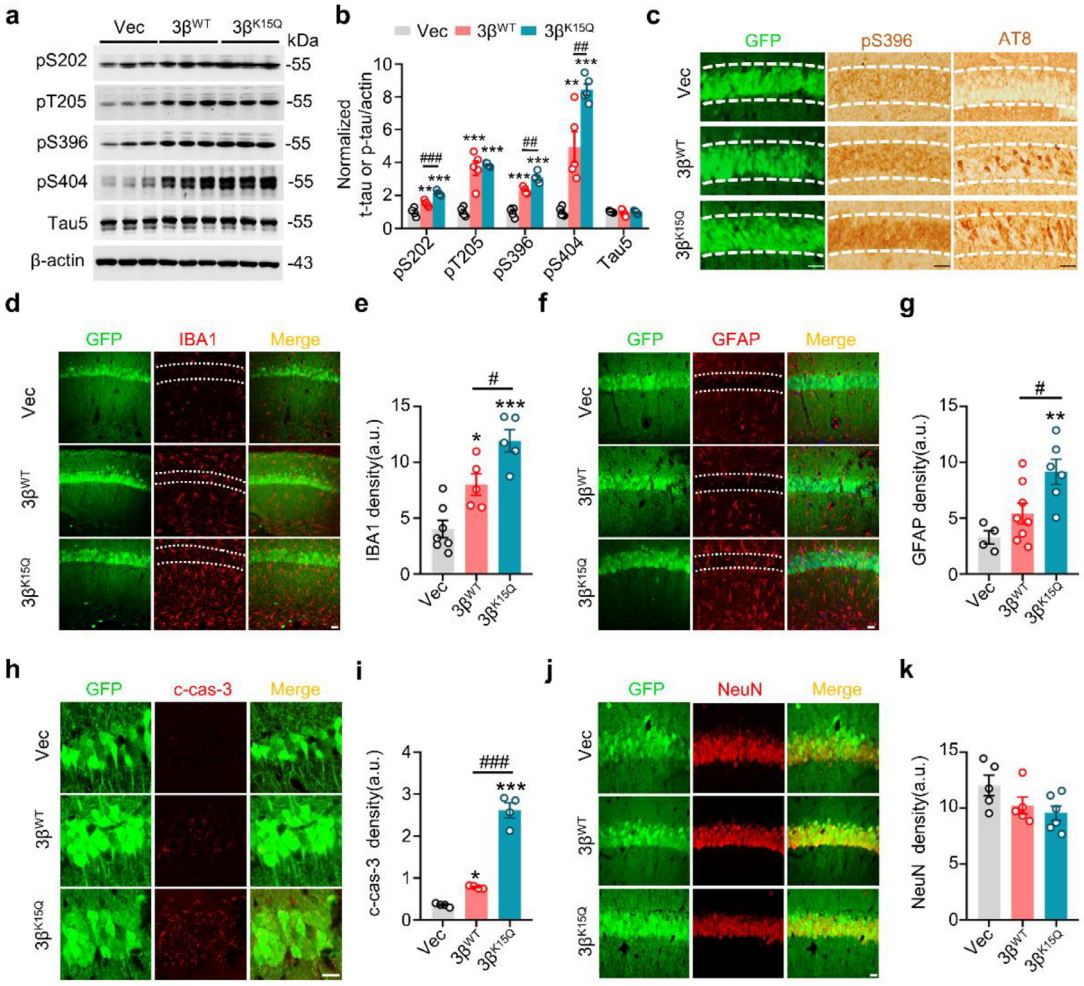

Figure 5. GSK-3β K15-acetylation exacerbates tau hyperphosphorylation with glial activation and neuron loss. (a–c) GSK-3β K15-acetylation exacerbated tau hyperphosphorylation at multiple AD-associated site compared with GSK-3β^{WT} measured by Western blotting (a,b) and Immunohistochemistry (c). (n = 5 for each group, one-way ANOVA, $^{**}p < 0.01$, $^{***}p < 0.001$ vs Vec, $^{\#\#}p < 0.01$, $^{\#\#\#}p < 0.01$ vs GSK-3β^{WT}, bar = 50 μm). (d–g) GSK-3β K15-acetylation exacerbated microglia (d,e) and astrocytes (f,g) activation compared with GSK-3β^{WT} measured by immunofluorescent staining using anti-IBA1 and anti-GFAP. (n = 4-8 for each group, one-way ANOVA, $^{*}p < 0.05$, $^{**}p < 0.01$, $^{***}p < 0.001$ vs Vec, $^{\#}p < 0.05$ vs GSK-3β^{WT}, bar = 20 μm). (h–k) GSK-3β K15-acetylation exacerbated apoptosis measured by cleaved caspase-3 (c-cas-3) immunofluorescent staining (h,i) with no significant influence on NeuN staining (j,k). (n = 4-6 for each group, one-way ANOVA, $^{*}p < 0.05$, $^{***}p < 0.001$ vs Vec, $^{\#\#\#}p < 0.001$ vs GSK-3β^{WT}, bar = 20 μm). Data were presented as mean ± SEM.

inactivated by its Ser9 phosphorylation.[36,47] We found that overexpressing tau increased protein level with increased Tyr216 phosphorylation and reduced Ser9 phosphorylation of GSK-3β without affecting its mRNA. Tau has acetyltransferase activity that can promote itself[38] and β-catenin acetylation.[39] To explore the intrinsic relationship between tau and GSK-3β during AD, we studied whether tau can directly acetylate GSK-3β and thus activate the kinase. As expected, overexpressing tau remarkably promoted GSK-3β acetylation with inhibited ubiquitination *in vitro*, and mutation of tau at its acetyltransferase activity region Tau-K18(-) abolished the effects. By incubating affinity-purified tau and the purified GSK-3β *in vitro*, we confirmed that tau could directly acetylate GSK-3β at K15.

Protein acetylation is regulated by histone acetyltransferases (HATs). Previous studies showed that histone acetylation was inhibited in tau-expressing cells.[52] We also observed that protein level of CBP and P300 was decreased in tau-overexpressing cells, furthermore, inhibiting the activity of CBP, P300 and PCAF did not attenuate the increased GSK-3β acetylation by tau. These data exclude the role of CBP, P300 and PCAF in promoting GSK-3β acetylation in our tau-overexpressing system, and confirm a predominant role of tau in acetylating GSK-3β.

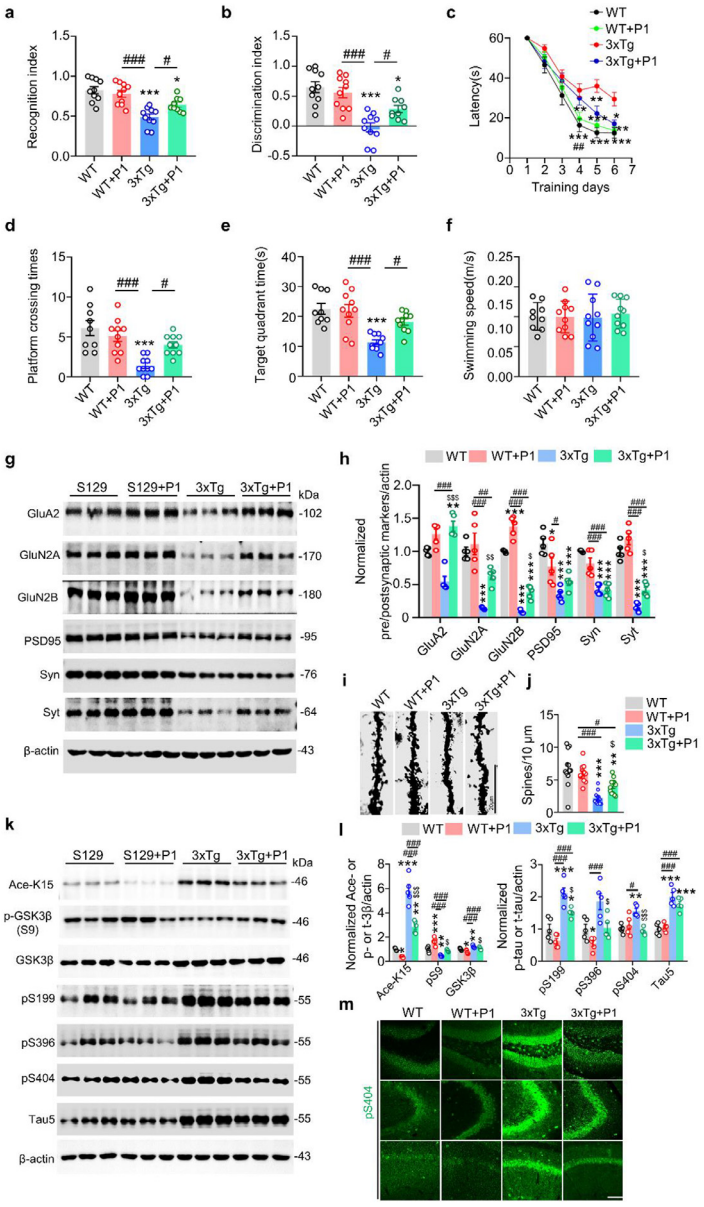

Figure 6. Blocking tau-induced GSK-3β acetylation by intracerebroventricular infusion of P1 attenuates the cognitive and synaptic deficits with reduced p-tau in 3xTg-AD mice. (a,b) Peptide 1 (P1) attenuated memory deficits of 3xTg-AD mice shown by the restored recognition index (a) and discrimination index (b) recorded at 24 h after training in novel object recognition test. (n = 9-10 for each group, one-way ANOVA, ***$p < 0.001$ vs WT, #$p < 0.05$, ###$p < 0.001$ vs 3xTg). (c−f) P1 alleviated the spatial learning deficit in 3xTg-AD mice shown by the decreased latency to find platform at days 5 and 6 during learning trial in Morris water maze test (c) (n = 9-10 for each group, Two-way ANOVA, *$p < 0.05$, **$p < 0.01$, ***$p < 0.001$ vs 3xTg, ##$p < 0.01$ vs 3xTg+P1), and P1 improved spatial memory shown by the increased platform crossings (d) and target quadrant time (e) during the probe trial, and there were no difference in swimming speed within the four groups (f). (n = 9-10 for each group, one-way ANOVA, ***$p < 0.001$ vs WT, #$p < 0.05$, ###$p < 0.001$ vs 3xTg). (g−h) P1 treatment increased levels of GluN2A, GluN2B, GluA2 and Syt in the hippocampus measured by western blotting. (n = 5 for each group, one-way ANOVA, *$p < 0.05$, **$p < 0.01$, ***$p < 0.001$ vs WT, #$p < 0.05$, ##p <0.01, ###p <0.001 vs WT+P1, $$p < 0.05$, $$$p < p < 0.01$, $$$$p < 0.001$ vs 3xTg). (i,j) P1 increased spine density in CA1 subset of 3xTg-AD mice measured by Golgi staining. (n = 12 neurons from 5 mice for each group, one-way ANOVA, **$p < 0.01$, ***$p < 0.001$ vs WT, #$p < 0.05$, ###$p < 0.001$ vs WT+P1, $$p < 0.05$ vs 3xTg, bar = 20 μm). (k−m) P1 attenuated phosphorylation and acetylation of GSK-3β and tau hyperphosphorylation in 3xTg-AD mice measured by Western blotting (k,l) and immunofluorescence (m). (n = 5 each group, one-way ANOVA, *$p < 0.05$, **$p < 0.01$, ***$p < 0.001$ vs WT, #$p < 0.05$, ###p <0.001 vs WT+P1, $$p < 0.05$, $$$$p < 0.001$ vs 3xTg, bar = 50 μm). Data were presented as mean ± SEM.

By proteomic analysis and site-specific mutagenesis, it was predicted that GSK-3β acetylation at K205 could regulate its enzyme activity.[37,53] In the present study, we found by mass spectrometry that overexpressing tau induced GSK-3β acetylation at N-terminal. Further studies by site-specific mutagenesis identified that the acetylation site of GSK-3β by tau was at K15 but not at K205 or K27. Then, we developed a specific antibody against K15-acetylated GSK-3β, and found that K15-acetylated GSK-3β was elevated in the brains of AD patients and AD transgenic mice. GSK-3β K15 can also be modified by ubiquitination.[54,55] We observed that overexpressing K15-acetylation mimics (GSK-3β^{K15Q}) reduced its ubiquitination with an inhibited degradation of GSK-3β. AKT and PKA can inhibit GSK-3β activity by phosphorylating the kinase at Ser9.[56,57] We found that expressing K15-acetylated GSK-3β also attenuated the phosphorylation of GSK-3β at Ser9. Together, the GSK-3β K15-acetylation by tau increases the kinase activity by stabilizing the protein and reducing its inhibitory phosphorylation at Ser9.

Tau phosphorylation enhances its acetyltransferase activity on self-acetylation or acetylating β-catenin.[38,39] We also observed that tau phosphorylation further promoted GSK-3β K15-acetylation and the K15-acetylation in turn increased the phosphorylation level of tau, forming a vicious cycle. This vicious cycle may explain the progressive exacerbation of AD pathologies. Previous studies also suggest that upregulating GSK-3β induces synapse damages and cognitive deficits, but the molecular mechanism is not fully understood. By overexpressing GSK-3β wild-type (GSK-3β^{WT}) or GSK-3β pseudo-acetylation (GSK-3β^{K15Q}) in mouse hippocampi, we observed that overexpressing GSK-3β^{WT} induced significant impairments of synaptic and cognitive functions with increased tau phosphorylation and glial proliferation, which were consistent with the previous reports.[8,15,58] We also found that expressing GSK-3β^{K15Q} induced severer neural toxicity than expressing GSK-3β^{WT}, which confirms the detrimental effects of GSK-3β K15-acetylation.

Importantly, we successfully developed a peptide that can competitively inhibit GSK-3β acetylation at K15 both *in vitro* and *in vivo*. Multiple-doses intracerebroventricular infusion of this peptide efficiently attenuated cognitive impairment and the AD-like pathologies in 3xTg-AD mice.

Together, we found in the present study that tau can directly acetylate GSK-3β at K15. GSK-3β K15-acetylation inhibits its ubiquitination and increases the activity of the kinase, which leads to synaptic dysfunction and memory deficit. Specific blocking the tau-induced GSK-3β K15-acetylation attenuates AD pathologies and improves the cognitive function. These findings reveal a novel vicious cycle between tau and GSK-3β in promoting AD progression.

Contributors

J-Z W and E L designed research; E L, Q Z, M L, S L, D K and Q W performed experiments; E L, Q Z, X-C W, Y Y, G-P L, and J-Z W analyzed data; J-Z W and E L verified data; J-Z W and E L wrote the manuscript. All authors read and approved the final manuscript.

Data sharing statement

All the data during the current study have been shown in manuscript and supplemental materials, and unprocessed data are available from the corresponding author on reasonable request.

Declaration of interests

The authors declare that they have no conflict of interest.

Acknowledgement

The authors thank Dr. Fei Liu of Jiangsu Key Laboratory of Neuroregeneration, Nantong for plasmids, and Dr. Chao Ma of Human Brain Bank, Chinese Academy of Medical Sciences for post-mortem human brain samples. This study was supported in parts by grants from Science and Technology Committee of China (2016YFC1305800), Hubei Province (2018ACA142), Natural Science Foundation of China (91949205, 82001134, 31730035, 81721005), Guangdong Provincial Key S&T Program (018B030336001).

Supplementary materials

Supplementary material associated with this article can be found in the online version at doi:10.1016/j.ebiom.2022.103970.

References

1 Llorens-Martin M, Jurado J, Hernandez F, Avila J. GSK-3beta, a pivotal kinase in Alzheimer disease. *Front Mol Neurosci*. 2014;7:46.
2 Platenik J, Fisar Z, Buchal R, et al. GSK3beta, CREB, and BDNF in peripheral blood of patients with Alzheimer's disease and depression. *Prog Neuropsychopharmacol Biol Psychiatry*. 2014;50:83–93.
3 Lauretti E, Dincer O, Pratico D. Glycogen synthase kinase-3 signaling in Alzheimer's disease. *Biochim Biophys Acta Mol Cell Res*. 2020;1867(5): 118664.
4 Ly PT, Wu Y, Zou H, et al. Inhibition of GSK3beta-mediated BACE1 expression reduces Alzheimer-associated phenotypes. *J Clin Invest*. 2013;123(1):224–235.
5 Uemura K, Kuzuya A, Shimozono Y, et al. GSK3beta activity modifies the localization and function of presenilin 1. *J Biol Chem*. 2007;282(21):15823–15832.
6 Sofola O, Kerr F, Rogers I, et al. Inhibition of GSK-3 ameliorates Abeta pathology in an adult-onset Drosophila model of Alzheimer's disease. *PLoS Genet*. 2010;6(9): e1001087.
7 Zhu LQ, Liu D, Hu J, et al. GSK-3 beta inhibits presynaptic vesicle exocytosis by phosphorylating P/Q-type calcium channel and interrupting SNARE complex formation. *J Neurosci*. 2010;30(10):3624–3633.

8 Zhu LQ, Wang SH, Liu D, et al. Activation of glycogen synthase kinase-3 inhibits long-term potentiation with synapse-associated impairments. *J Neurosci*. 2007;27(45):12211–12220.
9 Llorens-Martin M, Fuster-Matanzo A, Teixeira CM, et al. GSK-3beta overexpression causes reversible alterations on postsynaptic densities and dendritic morphology of hippocampal granule neurons *in vivo*. *Mol Psychiatry*. 2013;18(4):451–460.
10 Jo J, Whitcomb DJ, Olsen KM, et al. Abeta(1-42) inhibition of LTP is mediated by a signaling pathway involving caspase-3, Akt1 and GSK-3beta. *Nat Neurosci*. 2011;14(5):545–547.
11 Farr SA, Sandoval KE, Niehoff ML, Witt KA, Kumar VB, Morley JE. Peripheral administration of GSK-3beta antisense oligonucleotide improves learning and memory in SAMP8 and Tg2576 mouse models of Alzheimer's disease. *J Alzheimers Dis*. 2016;54(4):1339–1348.
12 Franklin AV, King MK, Palomo V, Martinez A, McMahon LL, Jope RS. Glycogen synthase kinase-3 inhibitors reverse deficits in long-term potentiation and cognition in fragile X mice. *Biol Psychiatry*. 2014;75(3):198–206.
13 Farr SA, Ripley JL, Sultana R, et al. Antisense oligonucleotide against GSK-3beta in brain of SAMP8 mice improves learning and memory and decreases oxidative stress: Involvement of transcription factor Nrf2 and implications for Alzheimer disease. *Free Radic Biol Med*. 2014;67:387–395.
14 King MK, Pardo M, Cheng Y, Downey K, Jope RS, Beurel E. Glycogen synthase kinase-3 inhibitors: Rescuers of cognitive impairments. *Pharmacol Ther*. 2014;141(1):1–12.
15 Hernandez F, Borrell J, Guaza C, Avila J, Lucas JJ. Spatial learning deficit in transgenic mice that conditionally over-express GSK-3beta in the brain but do not form tau filaments. *J Neurochem*. 2002;83(6):1529–1533.
16 Jope RS, Cheng Y, Lowell JA, Worthen RJ, Sitbon YH, Beurel E. Stressed and inflamed, can GSK3 be blamed? *Trends Biochem Sci*. 2017;42(3):180–192.
17 Fuster-Matanzo A, Jurado-Arjona J, Benvegnu S, et al. Glycogen synthase kinase-3beta regulates fractalkine production by altering its trafficking from Golgi to plasma membrane: implications for Alzheimer's disease. *Cell Mol Life Sci*. 2017;74(6):1153–1163.
18 Maixner DW, Weng HR. The role of glycogen synthase kinase 3 beta in neuroinflammation and pain. *J Pharm Pharmacol*. 2013;1(1):001. (Los Angel).
19 Knopman DS, Amieva H, Petersen RC, et al. Alzheimer disease. *Nat Rev Dis Prim*. 2021;7(1):33.
20 Weingarten MD, Lockwood AH, Hwo SY, Kirschner MW. A protein factor essential for microtubule assembly. *Proc Natl Acad Sci U S A*. 1975;72(5):1858–1862.
21 Cleveland DW, Hwo SY, Kirschner MW. Purification of tau, a microtubule-associated protein that induces assembly of microtubules from purified tubulin. *J Mol Biol*. 1977;116(2):207–225.
22 Arriagada PV, Growdon JH, Hedley-Whyte ET, Hyman BT. Neurofibrillary tangles but not senile plaques parallel duration and severity of Alzheimer's disease. *Neurology*. 1992;42(3 Pt 1):631–639.
23 Lin YT, Cheng JT, Yao YC, et al. Increased total TAU but not amyloid-beta(42) in cerebrospinal fluid correlates with short-term memory impairment in Alzheimer's disease. *J Alzheimers Dis*. 2009;18(4):907–918.
24 Thal DR, Holzer M, Rub U, et al. Alzheimer-related tau-pathology in the perforant path target zone and in the hippocampal stratum oriens and radiatum correlates with onset and degree of dementia. *Exp Neurol*. 2000;163(1):98–110.
25 Kimura T, Yamashita S, Fukuda T, et al. Hyperphosphorylated tau in parahippocampal cortex impairs place learning in aged mice expressing wild-type human tau. *EMBO J*. 2007;26(24):5143–5152.
26 Yin Y, Gao D, Wang Y, et al. Tau accumulation induces synaptic impairment and memory deficit by calcineurin-mediated inactivation of nuclear CaMKIV/CREB signaling. *Proc Natl Acad Sci U S A*. 2016;113(26):E3773–E3781.
27 Li X, Wang Z, Tan L, et al. Correcting miR92a-vGAT-mediated GABAergic dysfunctions rescues human tau-induced anxiety in mice. *Mol Ther*. 2017;25(1):140–152.
28 Li XG, Hong XY, Wang YL, et al. Tau accumulation triggers STAT1-dependent memory deficits by suppressing NMDA receptor expression. *EMBO Rep*. 2019;20(6).
29 Brier MR, Gordon B, Friedrichsen K, et al. Tau and Abeta imaging, CSF measures, and cognition in Alzheimer's disease. *Sci Transl Med*. 2016;8(338):338ra66.
30 Roberson ED, Scearce-Levie K, Palop JJ, et al. Reducing endogenous tau ameliorates amyloid beta-induced deficits in an Alzheimer's disease mouse model. *Science*. 2007;316(5825):750–754.
31 Vossel KA, Zhang K, Brodbeck J, et al. Tau reduction prevents Abeta-induced defects in axonal transport. *Science*. 2010;330(6001):198.
32 Li HL, Wang HH, Liu SJ, et al. Phosphorylation of tau antagonizes apoptosis by stabilizing beta-catenin, a mechanism involved in Alzheimer's neurodegeneration. *Proc Natl Acad Sci U S A*. 2007;104(9):3591–3596.
33 Vossel KA, Xu JC, Fomenko V, et al. Tau reduction prevents Abeta-induced axonal transport deficits by blocking activation of GSK3beta. *J Cell Biol*. 2015;209(3):419–433.
34 Suber T, Wei J, Jacko AM, et al. SCF(FBXO17) E3 ligase modulates inflammation by regulating proteasomal degradation of glycogen synthase kinase-3beta in lung epithelia. *J Biol Chem*. 2017;292(18):7452–7461.
35 Sutherland C, Leighton IA, Cohen P. Inactivation of glycogen synthase kinase-3 beta by phosphorylation: new kinase connections in insulin and growth-factor signalling. *Biochem J*. 1993;296(Pt 1):15–19.
36 Stambolic V, Woodgett JR. Mitogen inactivation of glycogen synthase kinase-3 beta in intact cells via serine 9 phosphorylation. *Biochem J*. 1994;303(Pt 3):701–704.
37 Monteserin-Garcia J, Al-Massadi O, Seoane LM, et al. Sirt1 inhibits the transcription factor CREB to regulate pituitary growth hormone synthesis. *FASEB J*. 2013;27(4):1561–1571.
38 Cohen TJ, Friedmann D, Hwang AW, Marmorstein R, Lee VM. The microtubule-associated tau protein has intrinsic acetyltransferase activity. *Nat Struct Mol Biol*. 2013;20(6):756–762.
39 Liu E, Zhou Q, Xie AJ, et al. Tau acetylates and stabilizes beta-catenin thereby promoting cell survival. *EMBO Rep*. 2020:e48328.
40 Garcia-Gorostiaga I, Sanchez-Juan P, Mateo I, et al. Glycogen synthase kinase-3 beta and tau genes interact in Parkinson's and Alzheimer's diseases. *Ann Neurol*. 2009;65(6):759–761. author reply 61-2.
41 Voss K, Gamblin TC. GSK-3beta phosphorylation of functionally distinct tau isoforms has differential, but mild effects. *Mol Neurodegener*. 2009;4:18.
42 Liu F, Tian N, Zhang HQ, et al. GSK-3beta activation accelerates early-stage consumption of hippocampal neurogenesis in senescent mice. *Theranostics*. 2020;10(21):9674–9685.
43 Liu E, Xie AJ, Zhou Q, et al. GSK-3beta deletion in dentate gyrus excitatory neuron impairs synaptic plasticity and memory. *Sci Rep*. 2017;7(1):5781.
44 Azevedo EP, Ledo JH, Barbosa G, et al. Activated microglia mediate synapse loss and short-term memory deficits in a mouse model of transthyretin-related oculoleptomeningeal amyloidosis. *Cell Death Dis*. 2013;4:e789.
45 Popp TA, Tallant C, Rogers C, et al. Development of selective CBP/P300 benzoxazepine bromodomain inhibitors. *J Med Chem*. 2016;59(19):8889–8912.
46 Moustakim M, Clark PG, Trulli L, et al. Discovery of a PCAF bromodomain chemical probe. *Angew Chem Int Ed Engl*. 2017;56(3):827–831.
47 Hughes K, Nikolakaki E, Plyte SE, Totty NF, Woodgett JR. Modulation of the glycogen synthase kinase-3 family by tyrosine phosphorylation. *EMBO J*. 1993;12(2):803–808.
48 Bhat RV, Shanley J, Correll MP, et al. Regulation and localization of tyrosine216 phosphorylation of glycogen synthase kinase-3beta in cellular and animal models of neuronal degeneration. *Proc Natl Acad Sci U S A*. 2000;97(20):11074–11079.
49 Li YC, Panikker P, Xing B, et al. Deletion of glycogen synthase kinase-3beta in D2 receptor-positive neurons ameliorates cognitive impairment via NMDA receptor-dependent synaptic plasticity. *Biol Psychiatry*. 2020;87(8):745–755.
50 Chien T, Weng YT, Chang SY, et al. GSK3beta negatively regulates TRAX, a scaffold protein implicated in mental disorders, for NHEJ-mediated DNA repair in neurons. *Mol Psychiatry*. 2018;23(12):2375–2390.
51 Beaulieu JM. A role for Akt and glycogen synthase kinase-3 as integrators of dopamine and serotonin neurotransmission in mental health. *J Psychiatry Neurosci*. 2012;37(1):7–16.
52 Chai GS, Feng Q, Wang ZH, et al. Downregulating ANP32A rescues synapse and memory loss via chromatin remodeling in Alzheimer model. *Mol Neurodegener*. 2017;12(1):34.

53 Song CL, Tang H, Ran LK, et al. Sirtuin 3 inhibits hepatocellular carcinoma growth through the glycogen synthase kinase-3beta/BCL2-associated X protein-dependent apoptotic pathway. *Oncogene*. 2016;35(5):631–641.

54 Akimov V, Barrio-Hernandez I, Hansen SVF, et al. UbiSite approach for comprehensive mapping of lysine and N-terminal ubiquitination sites. *Nat Struct Mol Biol*. 2018;25(7):631–640.

55 Udeshi ND, Svinkina T, Mertins P, et al. Refined preparation and use of anti-diglycine remnant (K-epsilon-GG) antibody enables routine quantification of 10,000s of ubiquitination sites in single proteomics experiments. *Mol Cell Proteom*. 2013;12(3):825–831.

56 Cross DA, Alessi DR, Cohen P, Andjelkovich M, Hemmings BA. Inhibition of glycogen synthase kinase-3 by insulin mediated by protein kinase B. *Nature*. 1995;378(6559):785–789.

57 Fang X, Yu SX, Lu Y, Bast RC, Woodgett JR, Mills GB. Phosphorylation and inactivation of glycogen synthase kinase 3 by protein kinase A. *Proc Natl Acad Sci U S A*. 2000;97(22):11960–11965.

58 Sen T, Saha P, Jiang T, Sen N. Sulfhydration of AKT triggers tau-phosphorylation by activating glycogen synthase kinase 3beta in Alzheimer's disease. *Proc Natl Acad Sci U S A*. 2020;117(8):4418–4427.